Spin−Spin Contributions to the Zero-Field Splitting Tensor in Organic Triplets, Carbenes and Biradicals—A Density Functional and Ab Initio Study

Sebastian Sinnecker

Max-Planck-Institut für Bioanorganische Chemie, Stiftstrausse 34-36, D-45470 Mülheim an der Ruhr, Germany

Frank Neese*

Lehrstuhl für Theoretische Chemie, Universität Bonn, Wegelerstrausse 12, 53115 Bonn, Germany

Received: July 10, 2006; In Final Form: August 31, 2006

An evaluation study for the direct dipolar electron spin−spin (SS) contribution to the zero-field splitting (ZFS) tensor in electron paramagnetic resonance (EPR) spectroscopy is presented. Calculations were performed on a wide variety of organic systems where the SS contribution to the ZFS dominates over the second-order spin−orbit coupling (SOC) contribution. Calculations were performed using (hybrid) density functional theory (DFT), as well as complete active space self-consistent field (CASSCF) wave functions. In the former case, our implementation is an approximation, because we use the two-particle reduced spin-density matrix of the noninteracting reference system. In the latter case, the SS contribution is approximated by a mean-field method which, nevertheless, gives accurate results, compared to the approximation free computation of the SS part in a CASSCF framework. For the case of the triplet dioxygen molecule, it was shown that restricted open-shell density functional theory (RODFT), as well as CASSCF, can provide accurate spin−spin couplings while spin-unrestricted DFT leads to much larger errors. Furthermore, 15 organic radicals, including several 1,3 and 1,5 diradicals, dinitroxide biradicals, and even a chlorophyll *a* model system, were examined as test cases to demonstrate the accuracy and efficiency of our approach within a DFT framework. Accurate *D* values with root-mean-square deviations of 0.0035 cm^{-1} were obtained. Furthermore, all trends, including those due to substituent effects, were correctly reproduced. In a different set of calculations, the polyacenes benzene, naphthalene, anthracene, and tetracene were studied. Applying DFT, the absolute *D* values were noticeably underestimated, but it was possible to correctly reproduce the trend to smaller *D* values with larger size of the systems. Finally, it was demonstrated that our approach is also well-suited for the study of carbenes. The smaller organic radicals of this work were also studied, through the use of CASSCF wave functions. This was a special advantage in the case of the triplet polyacenes, where the CASSCF approach gave better results than the DFT method. In comparing spin-restricted and spin-unrestricted results, it was shown through a natural orbital analysis and comparison to high-level ab initio calculations that even small amounts of spin polarization introduced by the unrestricted calculations lead to large deviations between the unrestricted Kohn−Sham (UKS) and restricted open-shell Kohn−Sham (ROKS) approaches. It is challenging to understand why the ROKS results show much better correlation with the experimental data.

1. Introduction

The zero-field splitting (ZFS) describes the interaction of unpaired electrons in the phenomenological spin-Hamiltonian approach to the analysis of magnetic data.[1] It is prominently met in transition-metal clusters[1−4] but is also of importance in organic triplet radicals. The ZFS is determined by the spin-Hamiltonian (SH) parameters *D* and *E*, which are necessary for an interpretation of magnetic resonance spectra.[5] Although it has been shown in the past that a reasonably accurate calculation of *g*-values, hyperfine coupling constants, and nuclear quadrupole data is already routinely possible with present-day density functional theory (DFT),[6,7] the challenge now is to develop, implement, and test similar approaches for an accurate and efficient computation of ZFS parameters. This paper is dedicated to this purpose.

So far, there are only a few methods available in the literature for the prediction of ZFS parameters with quantum chemical methods.[8−14] The applied ab initio approaches were shown to give very accurate ZFS parameters; however, the studies are limited to radicals of smaller size. The work of Havlas and Michel, based on the exact Breit−Pauli Hamiltonian for spin−orbit and spin−spin coupling, together with quasi-degenerate perturbation theory on top of CASSCF wave functions and CASPT2 energies may be particularly mentioned in this area.[10−12] Furthermore, Vahtras and co-workers discussed in a series of papers the spin−spin (SS) and spin−orbit (SO) contributions to the ZFS tensor, using multiconfigurational self-consistent field (MCSCF) wave functions.[15−17] Good accuracy was obtained for the investigated π-triplet radicals, and it was concluded that the SO contributions to the *D* parameter can be safely neglected.[15,17,18] To the best of our knowledge, the first calculation of the SS contribution using DFT was reported by Petrenko et al.[19] Recently, a DFT-based study on carbenes was published.[20]

In this work, we present the application of our recently implemented approach for the calculation of spin−spin (SS) contributions to the ZFS parameters.[3,21,22] This approach can

* Author to whom correspondence should be addressed. Tel.: +49-228-732351. Fax: +49-228-739064. E-mail: theochem@thch.uni-bonn.de.

10.1021/jp0643303 CCC: $33.50
Published on Web 10/14/2006

be widely used in combination with different quantum chemical methods, because the only required input is the one-electron spin-density matrix for the electronic state being investigated. In the case of a CASSCF wave function, this amounts to a simple mean-field approach.[22] However, prior to actual application studies, it is important to probe the accuracy of the applied method for systems for which accurate and reliable reference data are available. Such a study is reported below for a series of experimentally well-characterized organic radicals, where the SO contributions to the ZFS (not covered here) are expected to be negligible. A forthcoming paper will consider the contributions of the SS and SO parts to the ZFS parameters in transition-metal complexes in detail. Because it is not under dispute that high-level ab initio calculations can provide very accurate ZFS parameters, we have focused here on radicals of larger size to effectively take advantage of the moderate computational requirements of present-day DFT methods, in comparison to configuration interaction or coupled-cluster-based methods. However, the $^3O_2$ molecule was included in this study to discuss the performance of different methods over a larger region of internuclear distances, relative to literature results. Finally, complete active space self-consistent field (CASSCF) calculations were performed for a subset of the test molecules covered in this study.

Care was taken in this study to use functionals and basis sets that were similar to those typically used in the calculation of other spin Hamiltonian (SH) parameters. In this way, we want to support the choice of a consistent method that is well-suited for the calculation of all SH parameters.

2. Theory

A triplet radical with a total spin of $S = 1$ is characterized by three magnetic sublevels with $M_s = +1$, 0, and -1. While these levels are energetically degenerate within a nonrelativistic or scalar relativistic treatment, their degeneracy is lifted upon inclusion of spin−orbit and dipolar spin−spin couplings.[1,3,23] This effect is called zero-field splitting (ZFS), and it is parametrized by a matrix **D** within the phenomenological spin Hamiltonian:

$$\hat{H}_{\mathrm{ZFS}} = \hat{S}\mathbf{D}\hat{S} \tag{1}$$

In a coordinate system that diagonalizes **D**, the ZFS Hamiltonian can be rewritten as

$$\hat{H}_{\mathrm{ZFS}} = D\left[\hat{S}_z^{\,2} - \frac{1}{3}S(S+1)\right] + E[\hat{S}_x^{\,2} - \hat{S}_y^{\,2}] \tag{2}$$

with

$$D = D_{zz} - \frac{1}{2}(D_{xx} + D_{yy}) \tag{3}$$

and

$$E = \frac{1}{2}(D_{xx} - D_{yy}) \tag{4}$$

Hence, the ZFS is uniquely defined by the parameters D, E, and the tensor orientation. Typically, D and E/D are given in a coordinate system that fulfils the condition

$$0 \le E/D \le \frac{1}{3} \tag{5}$$

From first principles, the tensor **D** with elements D_{kl} contains four different contributions:[1,24,25]

$$D_{kl} = D_{kl}^{\mathrm{SS}} + D_{kl}^{\mathrm{SOC}(0)} + D_{kl}^{\mathrm{SOC}(-1)} + D_{kl}^{\mathrm{SOC}(+1)} \tag{6}$$

The spin−spin contribution $\boldsymbol{D}_{\mathrm{SS}}$ is a first-order term that is believed to usually dominate the ZFSs of organic radicals.[5] The three second-order spin−orbit coupling (SOC) contributions are important in transition-metal complexes and other systems with large SOC constants. In this work, they are neglected and preliminary test calculations indicate that this is, indeed, justified.

The Hamiltonian $\hat{H}_{\mathrm{SS}}$ that describes the SS contribution is given by

$$\hat{H}_{\mathrm{SS}} = \frac{g_e^{\,2}\alpha^2}{8}\sum_{i\neq j}\left[\frac{\hat{s}(i)\hat{s}(j)}{r_{ij}^{\,3}} - 3\frac{(\hat{s}(i)\mathbf{r}_{ij})(\hat{s}(j)\mathbf{r}_{ij})}{r_{ij}^{\,5}}\right] \tag{7}$$

Here, $\mathbf{r}_{ij} = \mathbf{r}_i - \mathbf{r}_j$ and $r_{ij} = |\mathbf{r}_i - \mathbf{r}_j|$ for electrons i and j at positions $\mathbf{r}_i$ and $\mathbf{r}_j$, and with spins $\hat{s}(i)$ and $\hat{s}(j)$. Furthermore, g_e is the free-electron g-value and α is the fine structure constant.

As a consequence of eq 7, the two-electron property D_{kl}^{SS} is dependent on the inverse third power of the interelectronic distance. This value is difficult to predict for short interelectronic distances, because wave functions built upon orbital products do not satisfy the interelectronic cusp conditions and this would seem to make an accurate calculation of D exceedingly complicated. However, it will be shown below that fairly reasonable results can already be obtained on the basis of rather moderate wave functions.

The spin−spin interaction term can be calculated as a first-order term from perturbation theory:[24]

$$D_{kl}^{\mathrm{SS}} = \frac{g_e^{\,2}\alpha^2}{4S(2S-1)}\left\langle \Psi_0^{\mathrm{SS}}\left|\sum_i\sum_{i\neq j}\frac{r_{ij}^{\,2}\delta_{kl} - 3r_{ij;k}r_{ij;l}}{r_{ij}^{\,5}}\{2\hat{s}_z(i)\hat{s}_z(j) - \hat{s}_x(i)\hat{s}_x(j) - \hat{s}_y(i)\hat{s}_y(j)\}\right|\Psi_0^{\mathrm{SS}}\right\rangle \tag{8}$$

Here, Ψ_0^{SS} denotes the $M_s = S$ component of the wave function for the state under investigation. This equation was implemented by Vahtras and co-workers employing multiconfigurational self-consistent field (MC−SCF) wave functions.[16] In this work, a different route is taken. The tensor components of $\mathbf{D}_{\mathrm{SS}}$ are calculated from the equation of McWeeny and Mizuno,[26]

$$D_{kl}^{\mathrm{SS}} = \frac{g_e^{\,2}\alpha^2}{4S(2S-1)}\sum_{\mu\nu}\sum_{\kappa\tau}\{P_{\mu\nu}^{\alpha-\beta}P_{\kappa\tau}^{\alpha-\beta} - P_{\mu\kappa}^{\alpha-\beta}P_{\nu\tau}^{\alpha-\beta}\} \times \langle\mu\nu|r_{12}^{\,-5}\{3r_{12;k}r_{12;l} - \delta_{kl}r_{12}^{\,2}\}|\kappa\tau\rangle \tag{9}$$

applying the spin density matrix $\mathbf{P}^{\alpha-\beta}$ from pure or hybrid DFT calculations and from CASSCF wave functions. For a Hartree−Fock wave function, this is an exact equation, because the two-particle spin-density matrix exactly factorizes in the indicated way. For DFT methods, the two-particle spin-density matrix is unknown and eq 9 refers to the noninteracting reference system instead. This is a commonly used procedure when it comes to two-electron observables in a DFT framework, and we presently see no practical alternative in the case of SS contributions to the ZFS. Finally, for multiconfigurational wave functions, eq 9 is an approximation in that the second-order spin-density matrix does *not* factorize in the indicated way. In fact, in this case, eq 9 corresponds to a mean-field approximation. Similar mean-

field approximations have been extremely successful for the spin−orbit coupling operator[27,28] where the two-electron part is treated to within 1% of its exact value by a mean-field approach. We have conjectured that an analogous situation is likely to exist for the SS part of the ZFS and provide below numerical evidence that this may indeed be the case. Additional evidence for the accuracy of the mean-field approximation in a multiconfigurational context was recently obtained in a detailed ab initio study of ZFS effects in atoms and diatomic molecules.[22]

3. Computational Details

A reasonably large number of different triplet species was compiled for the present study. These test systems were chosen from previous theoretical and experimental studies on ZFS parameters.[15,16,29−32] All molecules were geometry-optimized in their triplet states, using spin-unrestricted DFT. The pure BP density functional[33−35] was used in combination with the SV-(P) basis set.[36] Furthermore, the resolution of identity (RI) approximation was used,[37−40] together with the SV/J auxiliary basis set.[41]

The zero-field parameters D and E were obtained from additional single-point calculations, using the approach described in section 2. The performance of the pure BP density functional was tested in comparison to the B3LYP[42,43] hybrid functional together with unrestricted (e.g., UBP) and restricted open shell (ROBP, ROB3LYP) treatments. Furthermore, the EPR-II and EPR-III basis sets were used in single-point calculations.[44] They were developed for an accurate calculation of magnetic resonance parameters and are expected to also yield accurate ZFS data. However, to estimate the basis set limit, additional single-point calculations were performed for the $^3O_2$ molecule, using the extensive QZVP basis set.[45]

CASSCF calculations were performed for the $^3O_2$ molecule and for the smaller radicals in this study. The sizes of the active spaces were chosen based on a natural orbital analysis from prior individually selecting closed-shell coupled-electron pair (CEPA) calculations. Care was taken to choose the orbitals for the active spaces in a balanced way, e.g., all orbitals with occupation numbers between 1.98 and 0.02, or between 1.95 and 0.05, were included in the active spaces. The choice depended on the size of the systems and on the number of orbitals to be included in the active space. In most cases, the natural orbitals were determined to be very well-suited as initial orbitals for the CASSCF calculations. However, quasi-restricted orbitals from BP86 DFT calculations were also determined to provide good starting points and typically led to the same converged CASSCF solutions as the CEPA natural orbitals.

All calculations were performed with the ORCA electronic structure program.[46]

4. Results and Discussion

4.1. The Dioxygen Molecule. The first test case of this work was the $^3O_2$ molecule with an experimental ZFS parameter of $D = 3.96$ cm^{-1}.[47] This value contains noticeable SS and SO contributions.[16,22] As already noted, spin−orbit contributions were not covered in this work. As a consequence, we decided to compare our calculated D_{SS} values with the value calculated by Vahtras et al.[16] Using CASSCF wave functions, they obtained $D_{SS} = 1.44$ cm^{-1} at the equilibrium distance of 1.207 Å. Furthermore, they studied the dependence of D_{SS} on the nuclear distance R_{O-O} of $^3O_2$. To investigate the accuracy of our simplified mean field approach we have performed similar calculations. The distance dependence is shown in Figure 1 in comparison to the results of Vahtras et al. It is evident that the spin−spin contribution is distinctly overestimated, using unrestricted HF or DFT methods. In contrast, restricted open-shell density functional theory (RODFT) calculations and our CASSCF calculations with 12 electrons in 8 orbitals gave very consistent results, which are furthermore similar to the calculated CASSCF data from Vahtras et al., at least in the vicinity of the equilibrium distance. This comparison shows that (i) our mean field approach provided accurate results, in combination with CASSCF, and (ii) in DFT treatments, the RODFT method gives better results than spin-unrestricted treatments. However, for longer distances, a limited divergence was observed between our CASSCF results and those from Vahtras et al. This is attributed to a beginning breakdown of the mean field method as a consequence of the strongly increased static correlation effects that accompany bond breaking. In case of the DFT wave functions, a very small distance dependence of D_{SS} was obtained.

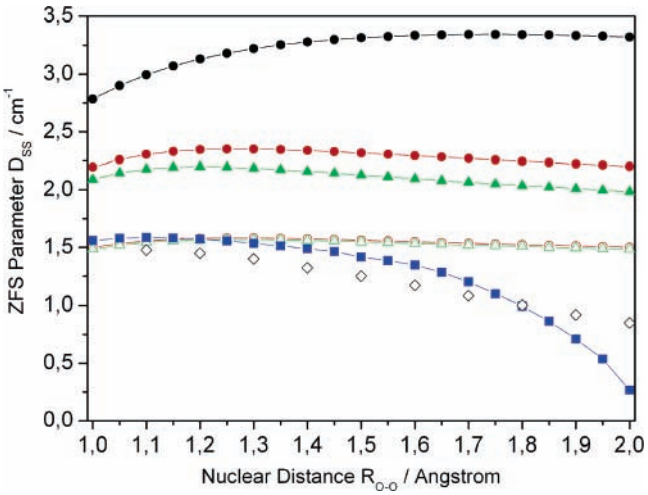

Figure 1. Calculated spin−spin (SS) contribution to the zero-field splitting (ZFS) parameter D for $^3O_2$ as a function of the nuclear distance employing the EPR-III basis set. Results are given for UHF (black circles), UB3LYP (red filled circles), UBP (green filled triangles), ROB3LYP (red open circles), ROBP (green open triangles), and CASSCF (blue squares). The diamonds indicate the CASSCF results from Vahtras et al., applying the aug-cc-pCVTZ basis set and 10 electrons in 12 orbitals. These values were estimated from Figure 2 in ref 16.

TABLE 1: Calculated Spin−Spin Contributions for the $^3O_2$ Molecule[a]

EPR-II			EPR-III			QZVP		
BP	B3LYP	CASSCF	BP	B3LYP	CASSCF	BP	B3LYP	CASSCF
1.52	1.53	1.55	1.57	1.58	1.57	1.58	1.59	1.57

[a] A value of $D_{SS} = 1.44$ cm^{-1} was calculated from Vahtras et al. at the equilibrium distance of 1.207 Å.[16] Our DFT calculations used restricted open-shell wave functions and the same bond distance. The CASSCF calculations were performed with an active space of 12 electrons in 8 orbitals.

A comparison of D_{SS} values calculated with different methods and basis sets is given in Table 1. In all cases, a equilibrium distance of 1.207 Å was used.[16] A value of $D_{SS} = 1.44$ cm^{-1} was obtained by Vahtras et al., using the aug-cc-pCVTZ basis set and an active space of 10 electrons in 12 orbitals. Our calculated values are somewhat larger (by 6%, up to 10%). A noticeable influence of the density functional or the basis set on the calculated values was not observed. The results with the QZVP basis set are expected to be similar to the basis set limit. Hence, the EPR-II and EPR-III basis sets can be safely used for calculations on larger molecules.

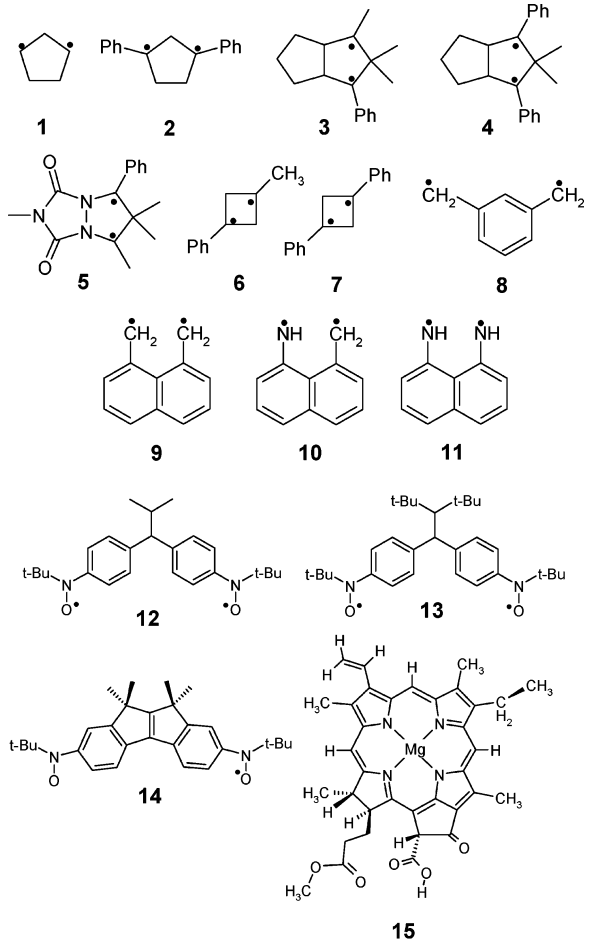

Figure 2. Structure and numbering of the triplet radicals used for the correlation of experimental with calculated *D* values in Figure 3.

4.2. Density Functional Calculations of Organic Radicals. *4.2.1. Organic Radicals with Small D Values.* In the next step of this work, a large number of organic radicals with zero-field splittings of $D < 0.10$ cm^{-1} were systematically studied. The performance of the BP functional, in combination with the EPR-II and EPR-III basis sets, was tested and compared with B3LYP/EPR-II calculations. The test molecules are given in Figure 2 (radicals **1**−**15**) and contain triplet species of different character. Strained rings, as well as conjugated and nonconjugated systems, were considered, in addition to radicals with and without heteroatoms. Even a chlorophyll *a* model system was included in this study (**15**). Despite the diversity of these radicals, care was taken that the chosen species show trends in their *D* values that must be correctly recovered if the proposed method is to be considered reliable.

The results are graphically displayed in Figure 3 by comparing experimental *D* values with calculated D_{SS} parameters. For systems **1**−**15**, it is assumed that the error due to the neglect of the SO contributions is small. It can be seen that a very good correlation with the experimental values was obtained in all three cases where restricted open-shell (RO) wave functions were used. Distinctly larger deviations between theory and experiment were obtained with the unrestricted UBP method. In the latter case, an overestimation of the *D* values was observed for all species, except the chlorophyll *a* model system (**15**).

The ROBP and ROB3LYP results will be analyzed in more detail. Comparing radicals **1** and **2**, a smaller *D* value was observed for the more-delocalized triplet species **2** in the experiments,[29,48] and this is well-reproduced by the DFT calculations. A similar trend was observed in the experiments and calculations for the 1,3 triplet diradicals **3**, **4** and **6**, **7**.[29,49] For radical **5**,[29] a slight underestimation was observed in the BP calculations.

For the series of radicals **8**−**11**, more-subtle changes in the experimental *D* values were reported.[50] The largest *D* value of this group was measured for radical **8** with its single benzene ring. This was also reproduced in the ROBP calculations. The smallest *D* value was measured and calculated for radical **9** with two benzene rings. Substituting the CH_2 fragment in radical **9** with one NH group (**10**) or two NH groups (**11**) resulted in larger *D* values, which was also observed in the calculations. The only qualitative difference in the ROBP and ROB3LYP results is the relative size of the *D* values in radicals **8** and **11**, because of an overestimation of *D* in radical **11**, using the ROB3LYP method.

In addition, it was also possible to accurately calculate the small *D* values for the nitroxide compounds **12**−**14** and their subtle changes with RODFT, in comparison to the experimental data.[32] For the chlorophyll (^{3}Ch1) *a* model system **15**, an underestimation of *D* was observed in all calculations, in comparison to the experimental value taken from Lendzian et al.[51]

Overall, a quite small root-mean-square deviation (RMSD) of 0.0035 cm^{-1}, which was observed between calculated and measured *D* values, was obtained with the BP functional in combination with the EPR-II basis set for radicals **1**−**15**. Results of similar accuracy were obtained with the EPR-III basis set (ROBP/EPR-III). However, the computational effort for the calculations with the EPR-III basis set is already rather high, especially for the larger radicals (**12**−**15**). The B3LYP hybrid functional (ROB3LYP/EPR−II) has a tendency to slightly overestimate the experimental *D* parameters.

For radicals **1**−**15**, only a few measured *E* values are available in the literature, which are all very small (<0.002). A comparison with the calculated data is given in the Supporting Information and shows that the *E* parameters are typically slightly overestimated. Furthermore, no noticeable influence of the functional or basis set on the calculated *E* values was observed.

4.2.2. Benzene and Polyacenes. An accurate reproduction of the experimental *D* values of benzene (0.159 cm^{-1}), naphthalene (0.1004 cm^{-1}), anthracene (0.0702 cm^{-1}), and tetracene (0.0573 cm^{-1})[52,53] turned out to be more problematic than for the radicals **1**−**15**. Although it was possible to calculate the *D* value of triplet benzene accurately, all DFT methods underestimated the *D* parameters of the polyacenes, almost by a factor of 2 (see Table 2).

TABLE 2: Comparison of Experimental and Calculated *D* Parameters for Benzene and Polyacenes

	BP/EPR-II	BP/EPR-III	B3LYP/EPR-III	experiment[52,53]
benzene	0.163	0.159	0.162	0.1593
naphthalene	0.053	0.052	0.051	0.1004
anthracene	0.042	0.042	0.041	0.0702
tetracene	0.032	0.031	0.032	0.0573

This is consistent with the finding of Loboda et al., that restricted open-shell Hartree−Fock (ROHF) calculations recover only one-half of D_{SS} in these systems.[15] Nevertheless, our DFT calculations provided slightly improved *D* values for benzene, naphthalene, and tetracene, compared to the ROHF values.

The discrepancy between measured and DFT-based *D* values in Table 2 indicates a limitation in the achievable accuracy in the case of aromatic hydrocarbons. However, the experimental

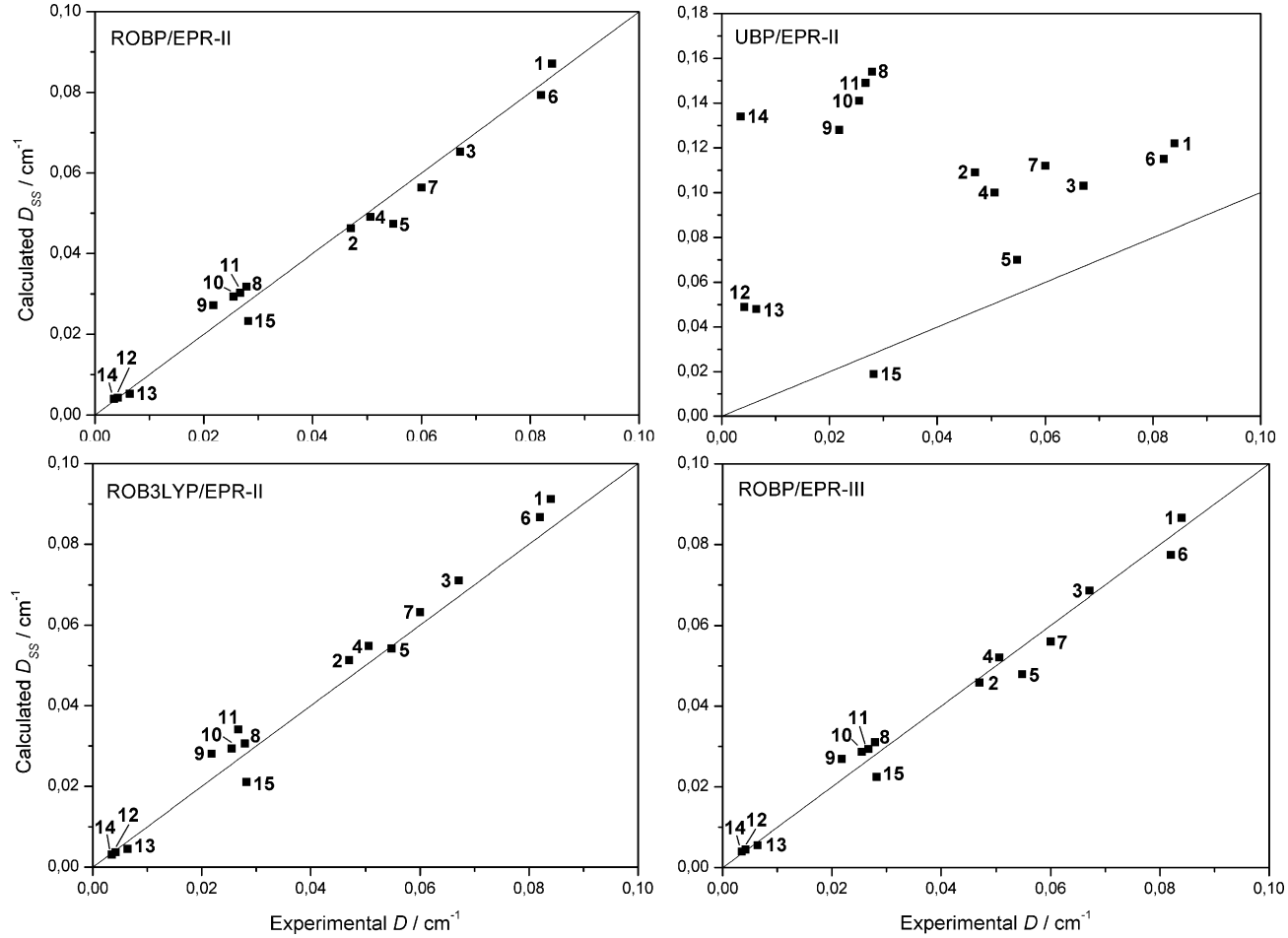

Figure 3. Correlation of calculated D_{SS} with measured D values for the organic radicals **1**−**15** from Figure 2. Comparison of restricted open-shell ROBP/EPR-II (top left), unrestricted UBP/EPR-II (top right), ROB3LYP/EPR-II (bottom left), and ROBP/EPR-III (bottom right) calculations. In all cases, single-point calculations on triplet-state geometries were performed. Root mean square deviation (RMSD) values of 0.0035 cm^{-1} (BP/EPR-II), 0.0772 cm^{-1} (UBP/EPR-II), 0.0035 cm^{-1} (BP/EPR-III), and 0.0045 cm^{-1} (B3LYP/EPR-II) were obtained.

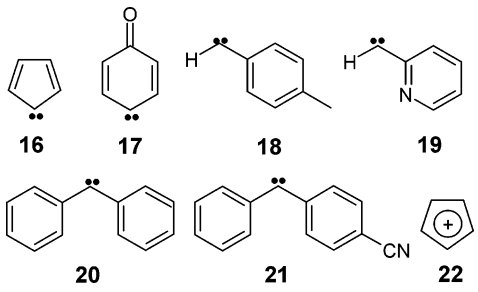

Figure 4. Structures and numbering of the triplet biradicals with larger D values.

trend to smaller D values with increasing size of the aromatic systems was well recovered. In section 4.3, it will be shown that the inclusion of static π-electron correlation at the CASSCF level improves the calculated D values of these aromatic molecules.

4.2.3. Organic Biradicals with Larger D Values. Finally, a group of triplet biradicals with larger D values was investigated (Figure 4). It contains six charge-neutral carbenes (**16**−**21**) and the triplet cyclopentadienyl cation **22**. Applying DFT, good agreement between theory and experiment was observed for the radicals **16**, **18**, and **19** (Table 3). The effect of the basis set on the calculated data is, again, small. However, in contrast to the radicals **1**−**15**, the B3LYP hybrid functional turned out to improve the calculated data, in comparison to the BP calculations (radicals **18**, **19**, **20**, and **21**).

Table 3 also shows calculated D parameters from a recent hybrid DFT study of Shoji et al., from which also most of the test systems from Figure 4 were taken.[20] These authors presented quite-accurate ZFS parameters and also included rather large systems in their study but restricted their work to biradicals. A comparison of the computed data with the experimental ones shows that our data are typically closer to the experimental results. However, it is interesting to note that the D values of our "problem cases" **17** and **22** were also considerably underestimated in the work of Shoji et al.

Furthermore, radicals **16**−**22** are well suited to probe the accuracy of the calculated E values since they were measured for all these systems and are distinctly larger than in the case of radicals **1**−**15**. Table S1 (Supporting Information) shows that the trends are correctly reproduced for most of the systems. More-accurate data were obtained from the BP calculations in comparison to the B3LYP results. Nevertheless, the relative errors in the calculation of E turned out to be distinctly larger than in the case of D.

4.3. Comparison with CASSCF Calculations. Finally, D values were calculated for 10 different radicals from this study, using CASSCF wave functions within the mean field approximation. For a better comparison with the DFT results, these calculations were also performed using the EPR-II basis set. Radicals from each group of sections 4.2.1, 4.2.2, and 4.2.3 were selected for that purpose; the results are given in Table 4.

TABLE 3: Comparison of Calculated with Measured D_{SS} Zero-Field Splitting Contributions[a]

	D_{SS} (cm^{-1})						
	16	**17**	**18**	**19**	**20**	**21**	**22**
BP/EPR-II	0.4120	0.2361	0.4722	0.5159	0.3288	0.2969	0.1356
BP/EPR-III	0.4181	0.2379	0.4711	0.5166	0.3294	0.2960	0.1327
B3LYP/EPR-II	0.4223	0.2314	0.4993	0.5441	0.3614	0.3354	0.1344
literature[b]	0.4412	0.2057	0.512	0.5443	0.3570		0.1269
experimental	0.4089[54]	0.3179[55]	0.516[56]	0.537[57]	0.408[30]	0.3906[30]	0.1868[58]

[a] The structures are displayed in Figure 4. [b] Theoretical results from Shoji et al.[20]

TABLE 4: Comparison of Calculated with Experimental *D* Values, Using CASSCF Wavefunctions[a]

	D value (cm^{-1})	
radical	CASSCF	experiment
1	0.081	0.084[29]
2	0.053	0.047[29]
8	0.027	0.0279[50]
benzene	0.146[b]	0.1593[52,53]
naphthalene	0.068[b]	0.1004[52,53]
anthracene	0.048[b]	0.0702[52,53]
tetracene	0.039[b]	0.0573[52,53]
16	0.585	0.4089[54]
17	0.339	0.3179[55]
22	0.141	0.1868[58]

[a] The following CAS spaces were used: **1**, (6,6); **2**, (4,4); **8**, (4,4); benzene, (6,6); naphthalene, (8,8); anthracene, (10,10); tetracene, (12,12); **16**, (4,4); **17**, (4,4); **22**, (4,5). The first number in parentheses denotes the number of active electrons; the second value refers to the number of active orbitals. [b] Loboda et al. calculated *D* values of 0.1591 cm^{-1} (benzene), 0.1142 cm^{-1} (naphthalene), 0.0836 cm^{-1} (anthracene), and 0.0564 cm^{-1} (tetracene), using ground-state geometries, RAS active spaces, and a double-ζ basis set.[15]

It is evident from the data that the multiconfigurational SCF approach can also give accurate ZFS parameters. Considering the radicals of the first group (**1**, **2**, and **8**), our CASSCF data are very similar to the experimental data, with deviations between 0.001 and 0.006 cm^{-1}. This indicates an accuracy similar to that observed in the DFT calculations. However, in the case of the polyacenes, the CASSCF calculations can play off their advantage of including static correlation. This is evident from our results in Table 4 and was already nicely demonstrated by the results from Loboda et al.[15] These authors found a strong dependence of *D* on the chosen geometry for naphthalene and obtained even better results than our data in Table 4. We have tried to produce results comparable to those by Lobodo et al., using ground-state optimized geometries for naphthalene at the BP/SV(P), RHF/6-31G, and CASSCF(10,10)/6-31G levels, together with several basis sets of double-ζ quality. However, our results proved to be stable against such variations with calculated *D* values in the range of 0.07−0.08 cm^{-1}. Because our CASSCF calculations in Table 4 were done with larger basis sets and larger active spaces, compared to the calculations of Loboda et al.,[15] it is likely that the mean-field approximation is responsible for the inferior quality of our results. At the same time, it appears that DFT, which covers short-range dynamic correlation effects well, also leads to significant errors. Thus, it seems that, in extended π-systems, there are strong static correlation effects that must be treated explicitly to arrive at accurate ZFS predictions. A more-detailed investigation seems to be necessary to develop further insight into this subject. Nevertheless, multideterminant approaches will probably be the methods of choice in this case. Note that it was not deemed necessary to include σ-MOs in the active spaces.[15]

In regard to the carbene radicals **16** and **17** with their large ZFS parameters, we observed *D* values in the CASSCF calculations that were too large, whereas the *D* parameter of the cyclopentadienyl cation **22** was underestimated. An accurate calculation of *D* in these biradicals is still a challenging task and somewhat larger deviations between theory and experiment must be tolerated. However, the calculations also faithfully reproduce the experimental trends.

Overall, the CASSCF values within the mean-field approximation for the ZFS parameters are not substantially more accurate than the DFT values. Therefore, the additional cost (presently, a factor of ∼2−10) of the CASSCF method, in comparison to DFT, is only well-invested under special circumstances. This may change after the exact SS treatment is implemented in our CASSCF program, as in the work of Vahtras, Minaev, and co-workers[15,17,18] and the program has reached the same level of optimization that the DFT module of the ORCA package already has.

4.4. Comparison of Spin-Restricted and Spin-Unrestricted Calculations. Perhaps the most surprising result of this study is the large discrepancy between the UKS and ROKS results. This is unexpected since spin contamination is not expected to be large for the chosen molecules. To obtain more insight into the origin of this effect, we have conducted a more-detailed comparison for a small molecule. We have chosen the first excited $^3(n \rightarrow \pi^*)$ state of H_2CO, because, in this case, a comparison to high-level ab initio calculations is possible. All calculations in this section were performed with the EPR-II basis set.

The energy of the $^3(n \rightarrow \pi^*)$ state was optimized at the UB3LYP level. Starting from the planar singlet geometry, the calculation converges to a planar saddle point with a single negative frequency of ∼640 cm^{-1}. Because the electronic structure of this state is more transparent for the present purposes than the nonplanar minimum energy structure, we have chosen to work with this structure rather than the genuine minimum energy structure. Naturally, the main geometric change, compared to the ground state, is the lengthening of the C═O bond from ∼1.2 Å to 1.31 Å in the $^3(n \rightarrow \pi^*)$ excited state.

The results of the computations are collected in Table 5. It is apparent that unrestricted Kohn−Sham (UKS) and restricted open-shell Kohn−Sham (ROKS), together with the B3LYP functional, lead to predictions of the *D* value that differ by a factor of ∼2. Therefore, the problem at hand is suitable to study the effect observed in the previous sections. It is first noted that the $\langle S^2 \rangle$ value of the UKS calculation is 2.0056, which is very similar to the expected value for a $S = 1$ state. Consequently, spin contamination should not be a major issue and the large discrepancy in the calculated *D* value is surprising. This is also apparent from the total energies of the UKS and ROKS calculations, which show that the UKS solution is <3 mEh lower in energy than the ROKS solution. Similarly, upon comparison of the Mulliken spin populations in the valence orbitals of the C and O atoms, it becomes apparent that the

TABLE 5: Comparison of Different Calculations on the First $n \rightarrow \pi^*$ Excited State of H_2CO at the UB3LYP Optimized Planar Saddle Point Geometry

	D (cm^{-1})[b]	E (cm^{-1})[b]	E_{tot} (E_h)[c]	$\rho(C_{2s})$[d]	$\rho(C_{2pz})$[d]	$\rho(C_{2px})$[d]	$\rho(C_{2py})$[d]	$\rho(O_{2s})$[d]	$\rho(O_{2pz})$[d]	$\rho(O_{2px})$[d]	$\rho(O_{2py})$[d]
UB3LYP	0.716	0.085	−1.3634	0.0363	0.7844	−0.0139	−0.0015	0.0080	0.1986	0.0017	0.8456
UNO−B3LYP	0.463	0.012	−1.3606	0.0000	0.7806	0.0000	0.0233	0.0000	0.1987	0.0000	0.8446
ROB3LYP	0.451	0.012	−1.3607	0.0000	0.7840	0.0000	0.0231	0.0000	0.1952	0.0000	0.8448
CASSCF[a]	0.506	0.045	−0.9156	0.0436	0.8227	−0.0139	−0.0035	0.0198	0.1526	0.0034	0.8888
MRMP2[a]	0.613	0.096	−1.1345	0.0669	0.8121	−0.0177	−0.0061	0.0172	0.1570	−0.0024	0.8803
MRMP3[a]	0.613	0.096	−1.1440	0.0669	0.8121	−0.0177	−0.0061	0.0172	0.1570	−0.0024	0.8803
MRMP4[a]	0.680	0.101	−1.1559	0.0614	0.7951	−0.0183	0.0019	0.0203	0.1728	−0.0020	0.8614
MRCI+Q[a]	0.695	0.104	−1.1557	0.0624	0.7928	−0.0183	−0.0056	0.0181	0.1761	−0.0016	0.8667
MRACPF[a]	0.731	0.115	−1.1551	0.0694	0.7844	−0.0192	−0.0120	0.0163	0.1825	−0.0014	0.8588

[a] All multireference calculations were based on a CASSCF calculation with 12 electrons in 11 orbitals. All post-CASSCF calculations were performed using $T_{pre} = 10^{-4}$ and $T_{Sel} = 10^{-12} E_h$. All electrons were correlated. MR−MPn results with nondiagonal and the CASSCF Fock operator definition of H_0. In fourth-order calculations, only singles and doubles were considered, as described by Grimme et al.[60] [b] The ZFS parameters were all calculated using eq 9 and the spin density calculated with the indicated method. For the multireference methods, the densities are "nonrelaxed" expectation value-like densities throughout. [c] Total energy + $113.0 E_h$. [d] Mulliken spin population. The molecule is lying in the *xy*-plane with the C═O bond placed along the *x*-axis.

spin distribution predicted by both calculations is fairly similar. All large positive values ($\rho(C_{2pz})$, $\rho(O_{2pz})$, $\rho(O_{2py})$) only differ in the third digit. The main differences in the two sets of numbers come from the small spin-populations ($\rho(C_{2s})$, $\rho(C_{2px})$, $\rho(C_{2py})$, $\rho(O_{2ps})$, $\rho(O_{2px})$), which must be attributed to spin polarization. To investigate whether these small differences already account for the considerable differences in the predicted D values, the UKS spin density was further analyzed. Using the spin-unrestricted natural orbitals (UNOs), the UKS spin density can be exactly written as a sum of two contributions: the first contribution stems from the leading spin-restricted determinant built from the first N_α UNOs (which is referenced as the "UNO" determinant; it is exactly equivalent to the "quasi-restricted" (QRO) determinant discussed recently[21]). Because the UNOs of a triplet state have the property that two UNOs are exactly singly occupied, these two UNOs define the spin density of the leading UNO determinant. The difference between this contribution and the full UKS spin density matrix define the spin-polarization contributions. The results obtained on the basis of the UNO determinant are also included in Table 5. It is obvious that the energy of the UNO determinant is almost indistinguishable from that of the ROKS solution, which justifies the statement made in ref 21 that these two determinants can be used almost interchangeably as long as $\langle S^2 \rangle \cong S(S+1)$. This is also shown by the calculated D value, which almost exactly equals the ROKS value. Thus, the large difference between the UKS and ROKS solutions must come from the minute amount of spin-polarization contained in the UKS determinant. This shows that the ZFS reacts extremely sensitively to the calculated spin distribution.

Because the ROKS values correlate better with the experimental values, the question arises whether the spin polarization predicted by the UKS calculations is unrealistic or, alternatively, whether the accuracy of the ROKS results stems from some type of error cancellation. To at least approximately address this question, several wave functions, which are expected to provide results similar to the full-CI limit in the EPR-II basis set, were calculated. The calculations were started from a CASSCF calculation of the $^3(n \rightarrow \pi^*)$ state with 12 electrons in 11 molecular orbitals, which comprises the full valence space of H_2CO. The starting orbitals for the CASSCF calculation were obtained from the (relaxed) natural orbitals of a spin-unrestricted MP2 calculation in a similar way, as advocated by Jensen et al.[59] Similar to the case of $^3O_2$, the mean-field CASSCF results for D are comparable to the RODFT numbers.

In the next step, dynamic correlation effects were taken into account by means of multiconfigurational Møller−Plesset (MP) perturbation theory up to fourth order (MRMP2−MRMP4), by multireference configuration (MRCI) and by the size-consistent MR averaged-coupled pair (MRACPF) variant. The dynamic correlation treatments are uncontracted; therefore, it is necessary to select the most important configuration state functions (CSFs) from the CASSCF solution, because it already consists of 98 010 CSFs with $S = 1$. Selecting all CSFs with a weight of at least 10^{-4} in the CASSCF solution leads to a set of 183 reference CSFs. From these, ∼21 million CSFs were generated in the first-order interacting space, of which 4.4 million were selected from the criterion that they have a second-order perturbation energy of at least 10^{-12} Eh with the 183-term reference wave function. All MR calculations were based on this set of 4.4 million selected CSFs. As it is evident from Table 5, the highest levels of theory (MRMP4, MRCI+Q, and MRACPF) all lead to essentially identical total energies which differ by <1 mEh. This energy is believed to be similar to the full CI energy of the $^3(n \rightarrow \pi^*)$ state in the EPR-II basis. We note, in passing, that an UCCSD(T) calculation gave an energy of −114.1514 Eh, which is only ∼4 mEh higher than the MR energies obtained here. Of the three most-accurate calculations, the highest credibility should perhaps be attached to the MRACPF calculation, because it is of infinite order in the treatment of electron−electron interaction (unlike MRMP*n* treatments) and it is size-consistent (unlike the MRCI solution). Despite the highly similar total energies, the spin populations predicted by the three methods still differ in subtle details. Based on the mean-field treatment, this translates to quite substantial differences in the predicted D value. Interestingly, the spin populations predicted by MRACPF are similar to those predicted by UB3LYP (note that the MRACPF solution strictly is a spin eigenfunction) and that the D values predicted by the two methods are also comparable. Note, however, that the mean-field MRACPF D value calculated here is, of course, not conclusive, with respect to the question of what would be obtained at the basis set and full-CI limits, together with an exact treatment of the SS operator. Such a study is unfortunately outside our present technical capabilities and definitely outside the scope of this investigation.

From the results previously described, it is concluded that the spin distribution predicted by the UB3LYP calculation is very realistic. This leaves us with the unsatisfactory situation that the UB3LYP calculations seemingly predict slightly better spin distributions than the ROB3LYP calculations but that the latter leads to predictions for D values that are in better agreement with the experimental data. It seems necessary to conclude that the high accuracy of the ROKS approach involves

a cancellation of errors that is, however, systematic. The *D* value was conclusively shown to be an extremely sensitive function of the calculated spin distribution. However, more-detailed insight into the origin of this effect must come from a much-more-detailed investigation, which is outside the scope of this work.

5. Conclusions

This work demonstrated the capability of density functional theory (DFT) and complete active space self-consistent field (CASSCF) for the calculation of spin−spin contributions to the zero-field splitting tensor. Our research was used to study the $^3O_2$ molecule and a significantly large number of organic radicals.

For the $^3O_2$ molecule, it was shown that, in a CASSCF framework, the mean-field approximation gave fairly accurate D_{SS} contributions. Results of comparable accuracy were obtained from RODFT wave functions, whereas unrestricted DFT calculations led to a significant overestimation of D_{SS}. In agreement with results obtained by Vahtras, Minaev, and co-workers,[15,17,18] it was determined that the basis-set dependence of the zero-field splitting (ZFS) at the CASSCF and DFT levels is moderate and that the EPR-II and EPR-III basis sets already provide results that are acceptably similar to the basis-set limit.

In the next step, a large set of organic radicals with small ZFS values was studied. The best correlation between calculated and experimental results was observed using ROBP calculations in combination with the EPR-II basis set. Therefore, this level of theory might be recommended for future studies. However, ROB3LYP is, at most, marginally inferior. An accurate calculation of *D* for aromatic triplet states was determined to be more challenging, as demonstrated for benzene, naphthalene, anthracene, and tetracene. Although the trend to smaller *D* values for the larger polyacenes was correctly reproduced, an underestimation of the experimental values was observed in our DFT calculations. Although we do not have a conclusive interpretation for this finding, it might be reasonable to speculate that the comparative failure of DFT might be related to the problems to describe electron-correlation effects at intermediate electron−electron distances, as has been shown recently by Grimme.[61] In these cases, multiconfigurational approaches should probably be applied to achieve a more quantitative agreement with the experimental data, in agreement with previous results.[15] Finally, several carbenes were studied. Again, a good correlation between experiment and theory was observed for the RODFT calculations. However, slightly larger deviations between theory and experiment were observed for this class of systems.

The large difference between RODFT and unrestricted density functional theory (UDFT) was an unexpected finding of the present work, and, therefore, some initial efforts have been made that may help to understand this effect. It was conclusively shown that the minute amounts of spin polarization are responsible for the large observed differences between the ROKS and UKS solutions and, consequently, the ZFS tensor reacts extremely sensitively to the calculated spin distribution. Through comparison with high-level ab initio calculations, it was argued that the UKS spin distribution is probably more realistic than the ROKS spin distribution, which is also the intuitively expected result in the case of small spin contamination. Therefore, it is likely that the good performance of the restricted open-shell Kohn−Sham (ROKS) method involves a certain amount of error compensation. However, at least in our opinion, the correlation with experiment is too systematic for the results assembled for organic radicals to be purely accidental. Consequently, more insight into this problem is required from future work.

This work demonstrated the possibility to study the ZFS of organic radicals based on DFT. Our approach allows the straightforward study of triplet states and diradicals in large biologically relevant molecules. Systems of the size of chlorophyll *a* were shown to be readily accessible with our program. Alternatively to this DFT based approach, ab initio methods based on multiconfigurational wave functions can be used for an accurate calculation of ZFS parameters. This was demonstrated in recent applications[15,16] and in this work. The drawback of these methods is their higher computational cost (depending on the size of the active space and the number of orbitals, CASSCF calculations may be 2−10 times more expensive than DFT calculations with the present version of the ORCA program). In addition, some workers would consider it a disadvantage that CASSCF calculations require additional insight from the user. The direct comparison of DFT and CASSCF results has shown, in many cases, similar or even more-accurate results within the DFT framework. Nonetheless, in situations with large medium- and long-ranged electron−electron correlation effects, ab initio methods will probably turn out to be preferable over DFT methods and, in our opinion, efforts toward their efficient development and implementation are well-invested.

A direct correlation between the ZFS parameters, which are integral properties of the radicals, and the electronic or even molecular structures of the investigated species is often difficult to achieve. Especially from this point of view, theoretical calculations might be helpful for a better understanding of these parameters. Future theoretical studies should also consider environmental effects on the ZFS parameters. This can include the use of continuum models, or the explicit inclusion of hydrogen bonds, as it was previously demonstrated for solvent shifts on electronic *g*-tensors.[62−64] A recent experimental study reported significant changes in the ZFS parameters caused by protic solvents.[65] In addition, many application studies for the calculation of ZFS parameters can be expected in the fields of bio-organic and bio-inorganic chemistry, where the inclusion of spin−spin contributions is also expected to be important.

Acknowledgment. This work has been supported by the Max Planck Society. Development of algorithms for Spin Hamiltonian parameter predictions are supported by a DFG grant to F.N. within the priority program "Molecular Magnetism", as well as the SFB 663 (University of Düsseldorf).

Supporting Information Available: Comparison of calculated (DFT) and measured *D* and *E* values for all organic radicals from this study. (PDF format.) This material is available free of charge via the Internet at http://pubs.acs.org.

References and Notes

(1) Neese, F. In *The Quantum Chemical Calculation of NMR and EPR Properties*; Kaupp, M., Bühl, M., Malkin, V. G., Eds.; Wiley: Heidelberg, Germany, 2004; p 541.

(2) Neese, F.; Solomon, E. I.; Miller, J. S.; Drillon, M. In *Magnetism: Molecules to Materials*; Wiley VCH: Weinheim, Germany, 2003; p 345.

(3) Neese, F. *Electron Paramagn. Reson.* **2006**, in press.

(4) Neese, F. *J. Biol. Inorg. Chem.* **2006**, *11*, 702−711.

(5) Schweiger, A.; Jeschke, G. *Principles of Pulse Electron Paramagnetic Resonance*; Oxford University Press: Oxford, U.K., 2001.

(6) Kaupp, M.; Bühl, M.; Malkin, V. G.; Eds. *Calculation of NMR and EPR Parameters. Theory and Applications*; Wiley−VCH: Weinheim, Germany, 2004.

(7) Neese, F. *Curr. Opin. Chem. Biol.* **2003**, *7*, 125.

(8) Minaev, B.; Tunell, I.; Salek, P.; Loboda, O.; Vahtras, O.; Agren, H. *Mol. Phys.* **2004**, *102*, 1391.
(9) Mählmann, J.; Klessinger, M. *Int. J. Quantum. Chem.* **2000**, *77*, 446.
(10) Havlas, Z.; Kyvala, M.; Michl, J. *Mol. Phys.* **2005**, *103*, 407.
(11) Havlas, Z.; Michl, J. *Perkin Trans.* **1999**, 2299.
(12) Havlas, Z.; Downing, J. W.; Michl, J. *J. Phys. Chem. A* **1998**, *102*, 5681.
(13) Minaev, B. F.; Khomenko, E. M.; Bilan, E. A.; Yashchuk, L. B. *Opt. Spectrosc.* **2005**, *98*, 209.
(14) Minaev, B.; Yaschuk, L.; Kukueva, V. *Spectrochim. Acta A* **2005**, *61*, 1105.
(15) Loboda, O.; Minaev, B.; Vahtras, O.; Schimmelpfennig, B.; Agren, H.; Ruud, K.; Jonsson, D. *Chem. Phys.* **2003**, *286*, 127.
(16) Vahtras, O.; Loboda, O.; Minaev, B.; Agren, H.; Ruud, K. *Chem. Phys.* **2002**, *279*, 133.
(17) Rubio-Pons, O.; Loboda, O.; Minaev, B.; Schimmelpfennig, B.; Vahtras, O.; Agren, H. *Mol. Phys.* **2003**, *101*, 2103.
(18) Loboda, O.; Tunell, I.; Minaev, B.; Agren, H. *Chem. Phys.* **2005**, *312*, 299.
(19) Petrenko, T. T.; Petrenko, T. L.; Bratus, V. Y. *J. Phys. Condens. Matter* **2002**, *14*, 12433.
(20) Shoji, M.; Koizumi, K.; Hamamoto, T.; Taniguchi, T.; Takeda, R.; Kitagawa, Y.; Kawakami, T.; Okumura, M.; Yamanaka, S.; Yamaguchi, K. *Polyhedron* **2005**, *24*, 2708.
(21) Neese, F. *J. Am. Chem. Soc.* **2006**, *128*, 10213.
(22) Ganyushin, D.; Neese, F. *J. Chem. Phys.* **2006**, *125*, 024103.
(23) Boca, R. *Coord. Chem. Rev.* **2004**, *248*, 757.
(24) Harriman, J. E. *Theoretical Foundations of Electron Spin Resonance*; Academic Press: London, 1978.
(25) Neese, F.; Solomon, E. I. *Inorg. Chem.* **1998**, *37*, 6568.
(26) McWeeny, R.; Mizuno, Y. *Proc. R. Soc. London* **1961**, *259*, 554.
(27) Hess, B. A.; Marian, C. M. In *Computational Molecular Spectroscopy*; Jensen, P., Bunker, P. R., Eds.; Wiley: New York, 2000; pp 169−219.
(28) Hess, B. A.; Marian, C. M.; Wahlgren, U.; Gropen, O. *Chem. Phys. Lett.* **1996**, *251*, 365.
(29) Adam, W.; Harrer, H. M.; Heidenfelder, T.; Kammel, T.; Kita, F.; Nau, W. M.; Sahin, C. *Perkin Trans.* **1996**, 2085.
(30) Akiyama, K.; Suzuki, A.; Morikuni, H.; Tero-Kubota, S. *J. Phys. Chem. A* **2003**, *107*, 1447.
(31) Prasad, B. L. V.; Radhakrishnan, T. P. *J. Mol. Struct. THEOCHEM* **1996**, *361*, 175.
(32) Shultz, D. A.; Boal, A. K.; Lee, H.; Farmer, G. T. *J. Org. Chem.* **1999**, *64*, 4386.
(33) Becke, A. D. *Phys. Rev. A* **1988**, *38*, 3098.
(34) Perdew, J. P. *Phys. Rev. B* **1986**, *34*, 7406.
(35) Perdew, J. P. *Phys. Rev. B* **1986**, *33*, 8822.
(36) Schäfer, A.; Horn, H.; Ahlrichs, R. *J. Chem. Phys.* **1992**, *97*, 2571.
(37) Dunlap, B. I.; Connolly, J. W. D.; Sabin, J. R. *J. Chem. Phys.* **1979**, *71*, 3396.
(38) Baerends, E. J.; Ellis, D. E.; Ros, P. *Chem. Phys.* **1973**, *2*, 41.
(39) Eichkorn, K.; Treutler, O.; Öhm, H.; Häser, M.; Ahlrichs, R. *Chem. Phys. Lett.* **1995**, *242*, 652.
(40) Eichkorn, K.; Weigend, F.; Treutler, O.; Ahlrichs, R. *Theor. Chem. Acc.* **1997**, *97*, 119.
(41) Eichkorn, K.; Treutler, O.; Öhm, H.; Häser, M.; Ahlrichs, R. *Chem. Phys. Lett.* **1995**, *240*, 283.
(42) Becke, A. D. *J. Chem. Phys.* **1993**, *98*, 5648.
(43) Lee, C. T.; Yang, W. T.; Parr, R. G. *Phys. Rev. B* **1988**, *37*, 785.
(44) Barone, V.; Chong, D. P. In *Recent Advances in Density Functional Methods*; World Scientific Publishing: Singapore, 1996; p 287.
(45) The basis sets can be downloaded from the ftp server of the Turbomole home page: http://www.turbomole.comH, 2003.
(46) Neese, F. *ORCA − an ab initio, Density Functional and Semiempirical Program Package*, Version 2.4, Max-Planck Institut für Bioanorganische Chemie, Mülheim an der Ruhr, Germany, 2004.
(47) Huber, K. P.; Herzberg, G. *Molecular Spectra and Molecular Structure, Constants of Diatomic Molecules*; van Nostrand Reinhold: New York, 1979.
(48) Adam, W.; Reinhard, G.; Platsch, H.; Wirz, J. *J. Am. Chem. Soc.* **1990**, *112*, 4570.
(49) Jain, R.; Sponsler, M. B.; Coms, F. D.; Dougherty, D. A. *J. Am. Chem. Soc.* **1988**, *110*, 1356.
(50) Berson, J. A. In *The Chemistry of Quinonoid Compounds*; Patai, S., Rappaport, Z., Eds.; Wiley: New York, 1988; Vol. II, p 462.
(51) Lendzian, F.; Bittl, R.; Telfer, A.; Lubitz, W. *Biochim. Biophys. Acta* **2003**, *1605*, 35.
(52) McGlynn, S. P.; Azumi, T.; Kinoshita, M. *Molecular Spectroscopy of the Triplet State*; Prentice Hall: Engelwood Cliffs, NJ, 1969.
(53) Clarke, R. H.; Frank, H. A. *J. Chem. Phys.* **1976**, *65*, 39.
(54) Wasserman, E.; Barash, L.; Trozzolo, A. M.; Murray, R. W.; Yager, W. A. *J. Am. Chem. Soc.* **1964**, *86*, 2304.
(55) Teki, Y.; Takui, T.; Itoh, K.; Iwamura, H.; Kobayashi, K. *J. Am. Chem. Soc.* **1986**, *108*, 2147.
(56) Chapman, O. L.; McMahon, R. J.; West, P. R. *J. Am. Chem. Soc.* **1984**, *106*, 7973.
(57) Chapman, O. L.; Sheridan, R. S.; LeRoux, J. P. *J. Am. Chem. Soc.* **1978**, *100*, 6245.
(58) Saunders, M.; Berger, R.; Jaffe, A.; McBride, J. M.; O'Neill, J.; Breslow, R.; Hoffman, J. M.; Perchonock, C.; Wasserman, E.; Hutton, R. S.; Kuck, V. J. *J. Am. Chem. Soc.* **1973**, *95*, 3017.
(59) Jensen, H. J. A.; Jorgensen, P.; Agren, H.; Olsen, J. *J. Chem. Phys.* **1988**, *88*, 3834.
(60) Grimme, S.; Parac, M.; Waletzke, M. *Chem. Phys. Lett.* **2001**, *334*, 99.
(61) Grimme, S. *Angew. Chem., Int. Ed.* **2006**, *118*, 4571.
(62) Rinkevicius, Z.; Telyatnyk, L.; Vahtras, O.; Ruud, K. *J. Chem. Phys.* **2004**, *121*, 5051.
(63) Sinnecker, S.; Rajendran, A.; Klamt, A.; Diedenhofen, M.; Neese, F. *J. Phys. Chem. A* **2006**, *110*, 2235.
(64) Minaev, B.; Loboda, O.; Vahtras, O.; Ruud, K.; Agren, H. *Theor. Chem. Acc.* **2004**, *111*, 168.
(65) Ehara, T.; Akiyama, K.; Ikoma, T.; Ikegami, Y.; Terokubota, S. *J. Phys. Chem.* **1995**, *99*, 2292.